IJST, Transactions of Mechanical Engineering, Vol. 36, No. M2, pp 143-153
Printed in The Islamic Republic of Iran, 2012

EXPERIMENTAL INVESTIGATION OF THE AIRFLOW AROUND SUPPORTED AND SURFACE MOUNTED LOW RISE RURAL BUILDINGS*

S. S. MOTALLEBI HASANKOLA, E. GOSHTASBI RAD AND O. ABOUALI**
School of Mechanical Engineering, Shiraz University, Shiraz, I. R. of Iran
Email: abouali@shirazu.ac.ir

Abstract– In this study, the flow around a rural building for both supported and surface mounted cases has been investigated. For this purpose experimental studies are performed. Hot wire anemometry was used to measure the stream-wise velocity in the wind tunnel. The experimental data depict that no recirculation zone exists in front of the supported building and the reattachment length behind this building decreases compared with that for the surface mounted building. Turbulent intensity was also measured and its variation around both building models is compared.

Keywords– Building, wind tunnel, hot-wire anemometer, turbulence

1. INTRODUCTION

The low rise buildings are very common in rural areas located in desert regions of Iran. The accumulation of the dust and sand around these buildings is a main issue and the first step for the analysis of this concern is to investigate the related flow field.

The flow field around the building has important effects on the wind loading, particle deposition and pollution distribution. Many researchers investigated the flow field around the various types of buildings and bluff bodies experimentally in the wind tunnels with smoke visualization, pressure transducer, hot film (or wire) anemometer, LDV and PIV instruments [1-7] in previous decades. Also, the flow field has been simulated numerically using different turbulence models [8-9].

Due to lack of large tunnels and advanced computers in the middle of the twentieth century, researchers faced a big challenge in both experimental and numerical simulations for the high Reynolds number flows. Townsend [10] suggested that the flow field is independent of Reynolds number for sufficiently high Reynolds numbers. This hypothesis is called Reynolds number similarity or Reynolds independency and nowadays, there is a great deal of experimental evidence to support this assumption [11-12]. Snyder [13] analyzed the independency range for Reynolds and Rossby numbers between the model and prototype.

To investigate a real situation, a thick boundary layer must be generated in the wind tunnel. Many researchers have presented different methods for boundary layer generation [14-17]. Counihan [16] presented a proper method to generate a thick boundary layer profile in small wind tunnels using a set of elliptic wedges and barriers. Also, he investigated the effect of barrier height and shape of elliptic wedge on boundary layer thickness in the wind tunnel.

Castro and Robins [3] measured the flow field around a cube in thin and thick boundary layers using pulsed wire and pressure transducer. They also investigated the flow field for different angles of

*Received by the editors August 17, 2011; Accepted September 25, 2012.
**Corresponding author

approaching flow such as 0, 22.5 and 45°. Meng and Hibi [18] measured three-dimensional components for mean and fluctuating velocities around a high rise building at Reynolds number of 2×10^4 using a split- fiber probe.

As the literature survey has shown, there is a lack of data for the flow field around the low rise rural buildings. Investigation of the flow field around these types of buildings is the main aim of the present work. In addition, the flow around a supported low rise building is studied. This supported building may be a way to prevent the accumulation of the dust and sand around rural buildings in desert regions. As the wind can pass through under the building it may transport the dust, and sands away from around the building. In the present study, the velocity and turbulence intensity ($\frac{u_{RMS}}{Uref}$) were measured experimentally by hot wire anemometer around a surface mounted low rise building and a building with four supports.

2. EXPERIMENTAL APPARATUS AND PROTOTYPE CONSTRUCTION

The experiments were conducted in a low speed, blowing type, open-circuit wind tunnel in the school of mechanical engineering in Shiraz University. This tunnel has a square cross section of 46cm×46cm and a length of 289 cm. The velocity in the tunnel is controlled using a frequency inverter and the maximum design wind speed is almost 32 m/s. The velocities selected for the present experiments are in the range of 10-15 m/s.

This tunnel was used before for the measurement of two dimensional flows over a blunt plate and around a hemisphere with thin and thick inflow boundary layers [19-20]. The velocity field measurements are done by three dimensional traversing hot-wire system installed by Fara Sanjesh Saba Co. (FSS), which is used to move the hot wire probes automatically. This mechanism is composed of a lead screw driven by a micro computer controlled stepper motor. The stiffness of the mechanism was also checked to ensure that no flow induced vibrations occurred. In all regions, split fiber hot wire probes by DANTEC Co. were used to measure the mean and fluctuation velocities around the building model. The used probe consists of two parallel nickel films deposited on the same quartz fiber with a length of 3 mm and diameter of 220 μm. The ends of the fiber are copper and gold-plated, leaving a 1.2 mm sensing length. Also, the film is protected with a 0.5 μm quartz coating. Split-fibers are designed for measurement of instantaneous velocity in gas flows [21]. This probe consists of two separated similar half-cylinder thin films and can detect the flow direction. The half-cylinder which is against the flow direction dissipates more heat compared with the other one; as a result, this probe can be efficient for the measurement in the flow field with recirculation regions which experience a change in the flow direction. This bi-directional split fiber probe operates with a constant temperature anemometer (CTA) bridge to measure the velocity in the reverse-flow regions [21]. The probe was calibrated in the tunnel by Karman-vortex method using Roshko's correlation. Roshko [22] showed that for a cylinder located in the free stream flow in the range of 50<Re<2000, the flow field in downstream region has a sinusoidal pattern. He also presented a relation for vortex shedding frequency as a function of Re number as follows,

$$\begin{cases} F = 0.212\mathrm{Re} - 4.5 & (50 < \mathrm{Re} < 150) \\ F = 0.212\mathrm{Re} - 2.7 & (300 < \mathrm{Re} < 2000) \end{cases} \quad (1)$$

In this relation F is a non-dimensional frequency and is equal to fd^2/υ, where d is the cylinder diameter, f is the vortex frequency and υ is the kinematic viscosity. Ardekani [23] presented the details of Karman-vortex calibration method. Based on his procedure, the probe must be located at a suitable distance from the cylinder. In this study a cylinder with a 1.9 mm diameter and 45 cm length was used to create regular vortexes. During experiments, the temperature of the air inside the wind tunnel varied between 20–22 $^\circ$C.

The sizes of the common rural buildings are assumed to be about 10 meters in length, 10 meters in width and 3 meters in height. In addition, the bases for the supported building were assumed to be 1 meter high and 0.4 meter in width and length. Reynolds number for this model was computed based on the building height and 10 m/s free stream velocity is almost 1.7×10^{6}, which is a high Reynolds number. Using the results of previous studies [10], for the Reynolds number independency the building model was constructed with a scale of $\frac{1}{100}$ which leads to a Reynolds number equal to 1.7×10^{4}. The building model was made of wood and then smoothed and colored. The models blockage ratios, a ratio of the cross sectional area of bluff body over the cross sectional area of the wind tunnel in the tunnel are almost 1.2%, which is in the acceptable range [24, 25]. Although the blockage ratio is in the acceptable range, the width of the building is a little high. There was a limitation for using a smaller width because of the Reynolds number independency and also criterion for the non-dimensional Jenson number (ratio of roughness of tunnel's surface over height of the building), which should be less than 0.001. Using a barrier and seven elliptic wedges as vorticity generators (Fig. 1) a boundary layer was generated thicker than the building height (almost four times). Figure 2a shows the generated boundary layer at a distance nearly 50H (H is the height of the surface mounted building model) from the tunnel inlet and 6.66 H upstream of the buildings which is in close agreement with the power law formula ($\frac{u}{U_{ref}}=\left(\frac{y}{\delta}\right)^{\frac{1}{8}}$). Also, Fig. 2b shows the inlet profile for root mean square (RMS) of velocity fluctuation in stream -wise direction, which has an average of 1.9%. at this location.

Fig. 1. Barrier and elliptic wedges at the inlet of the wind tunnel for thick boundary layer generation

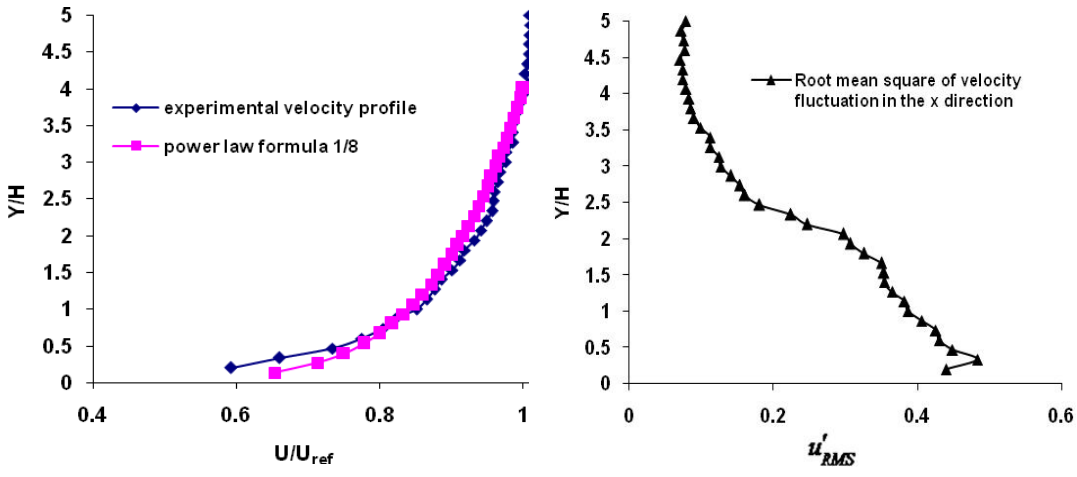

(a) (b)

Fig. 2. (a) Normalized mean velocity and (b) RMS of velocity fluctuation (m/s) in stream-wise direction at distance of 6.66H upstream of the building models

3. RESULTS

For the flow field with a thick boundary layer, the stream-wise velocity was measured around the surface mounted and supported buildings. Figure 3 shows a schematic of the supported building, wind direction and the symmetry plane. The stream-wise velocity measurement was done at the symmetry plane (Z/H=0) and a horizontal plane with Y/H=0.5 for surface mounted building and Y/H=0.833 for supported buildings. These horizontal planes correspond to the middle height of the buildings. Figures 4a and 4b show the distribution of stream-wise velocity around the surface mounted building respectively for X/H<3 and X/H>3. In these figures, horizontal and vertical axes show the non-dimensional distances of the measuring points, located in the shown vertical lines, from the reference of coordinates. Vertical dash lines represent the plotting lines. For evaluation of the measured stream-wise velocity, non-dimensionalized by U_{ref}, the distances between velocity profiles and corresponding plotting lines should be calculated based on the scale shown in the figure. The system coordinate is located on the symmetry plane and at the front of the model on the floor. Previous researches have shown that at the front, top and back of a surface mounted building, there exist reverse flow regions whose reattachment lengths depend on the aspect ratio, angle approaching of flow relative to body, type of boundary layer and also turbulence intensity [3, 18, 26-27]. To calculate the reattachment lengths, two following plotting lines (their closest measuring points to the surface show reverse directions for the stream-wise velocity) are recognized. The reattachment length is computed with interpolation between X/H values of the two mentioned plotting lines for the velocity of zero. The experimental data shown in Fig. 4 indicate that the recirculation zone in front of the surface mounted building is equal to X_f/H =1. The reattachment lengths at the roof and back of the building are equal to X_t/H =0.533 and X_r/H=2.44 respectively.

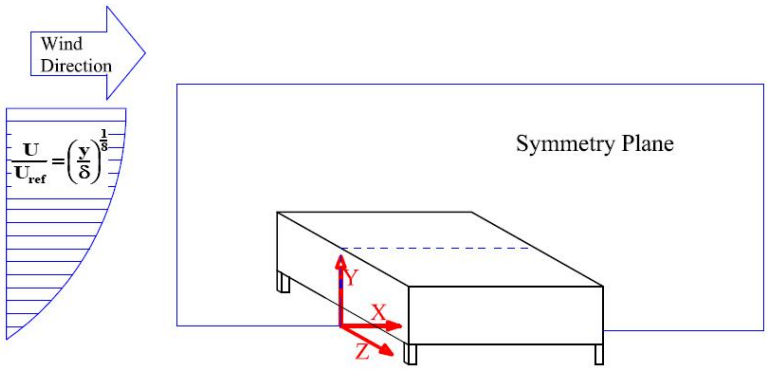

Fig. 3. Symmetry plane and wind direction for supported building

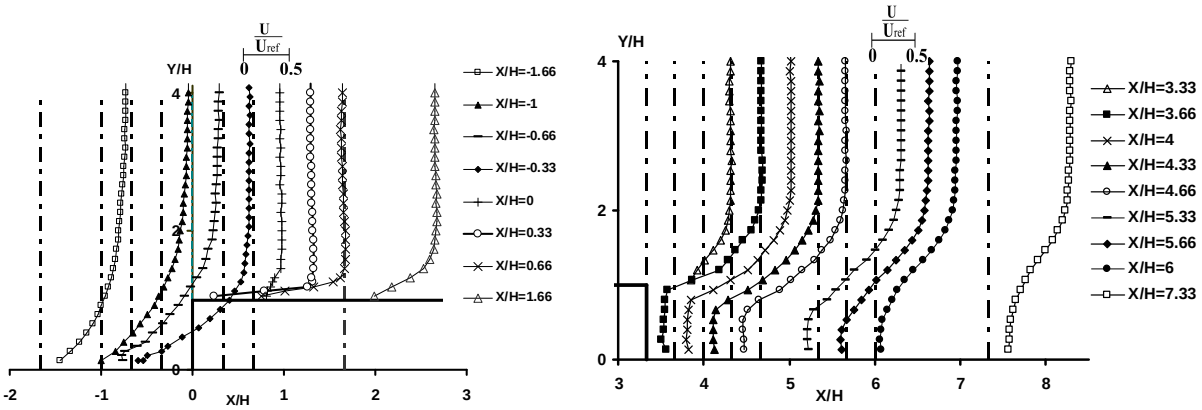

a) X/H<3 b) X/H>3

Fig. 4. Distribution of stream-wise velocity around surface mounted building at the symmetry plane (Z/H=0) for free stream velocity of 10 m/s

Because the turbulent intensity plays an important role on the pollution dispersion, this factor was also measured and then compared between the surface mounted and supported buildings. Figures 5a and 5b show turbulence intensity in the plane of symmetry. Turbulence intensity increases near the building front compared to the inlet of domain. These figures indicate that the turbulence intensity has a maximum near to the walls which decays when approaching the free stream regions. On the other hand, maximum values of turbulence intensity almost occur at the locations of the maximum stream-wise velocity gradient and shear layer thickness. The height of location for the maximum turbulence intensity increases in stream-wise direction at the roof while it decreases at the back of the building. These features were also observed around a hemisphere [24]. The maximum value of turbulence intensity behind the building is almost 0.11.

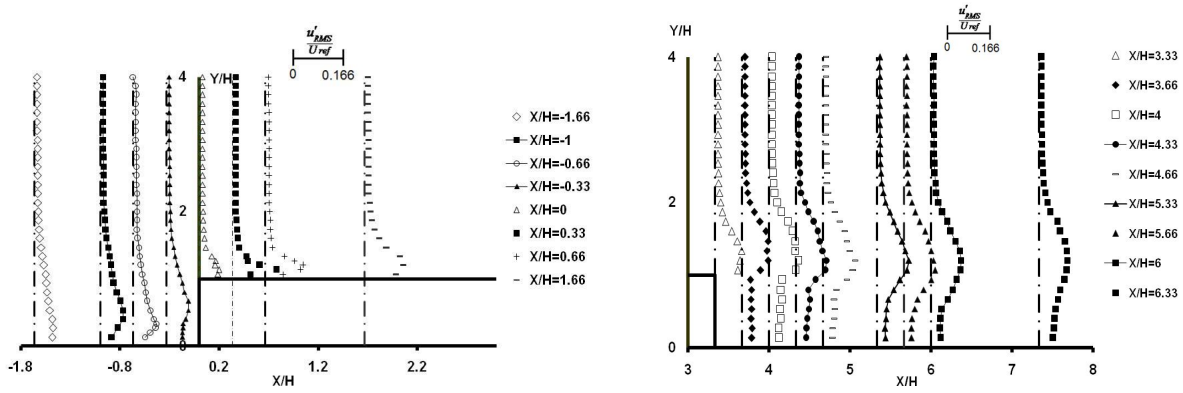

a) X/H<3 b)X/H>3

Fig. 5. Distribution of turbulence intensity around surface mounted building at the symmetry plane (Z/H=0) for free stream velocity of 10 m/s. (Plot lines are the same as Fig. 4)

Figure 6 compares the distribution of the stream-wise velocity for two Reynolds numbers of 17000 and 25000. The flow fields for both Reynolds numbers have nearly the same reattachment lengths and velocity distributions. Figures 7a and 7b show the comparison of the turbulence intensity for the two mentioned Reynolds numbers. As the results depicting the turbulence intensity are the same for both Reynolds numbers, this confirms that the Reynolds number of 17000 can be considered in the range of Reynolds number independency.

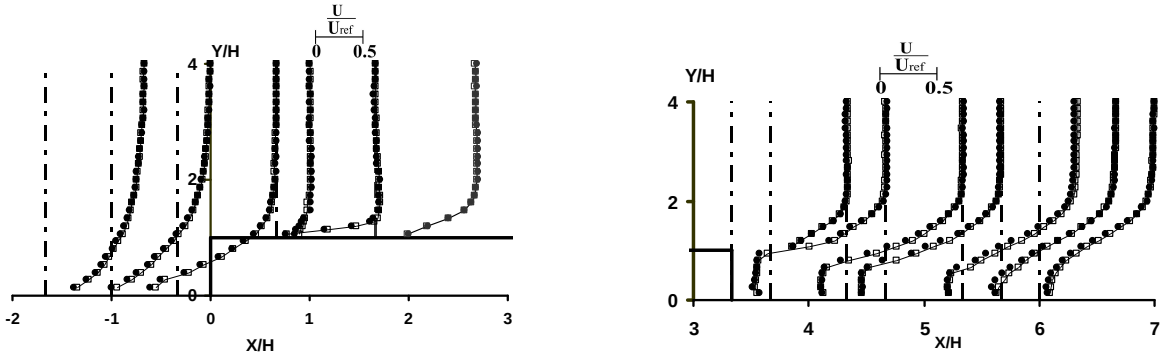

a) X/H<3 b) X/H>3

Fig. 6. Distribution of stream-wise velocity around surface mounted building at the symmetry plane (Z/H=0) for free stream velocities of 10 m/s (●) and 15 m/s (—□—)

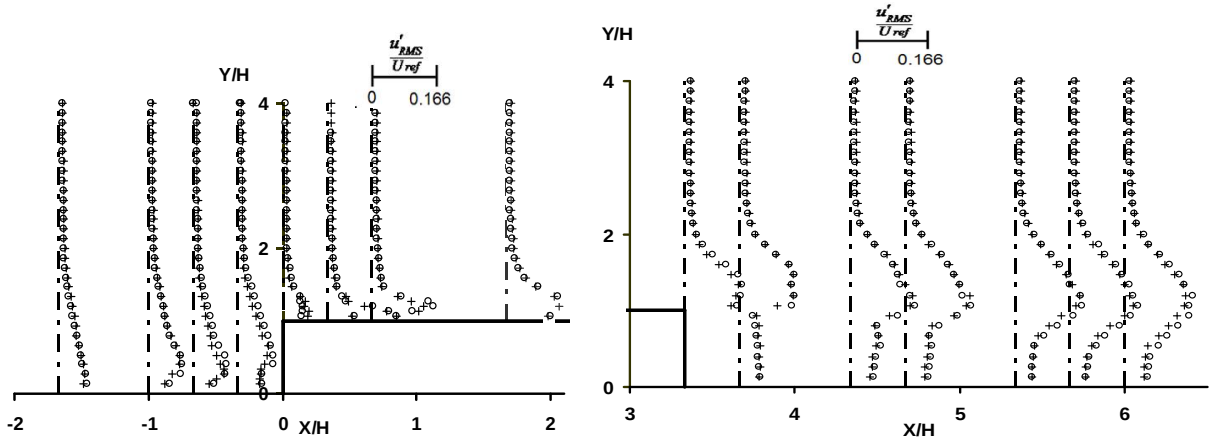

a) X/H<3 b) X/H>3

Fig. 7. Distribution of turbulence intensity around surface mounted building at the symmetry plane (Z/H=0) for free stream velocities of 10 m/s (+) and 15 m/s (O)

Figure 8 shows the distribution of stream-wise velocity in a horizontal plane at Y/H=0.5 (half of the surface mounted building height). At this height, the recirculation zone in front of the building does not exist, which indicates the stagnation point is close to the floor. But reverse flow at the back of the building still exists. Also, at the side of the building a small reverse zone is detected.

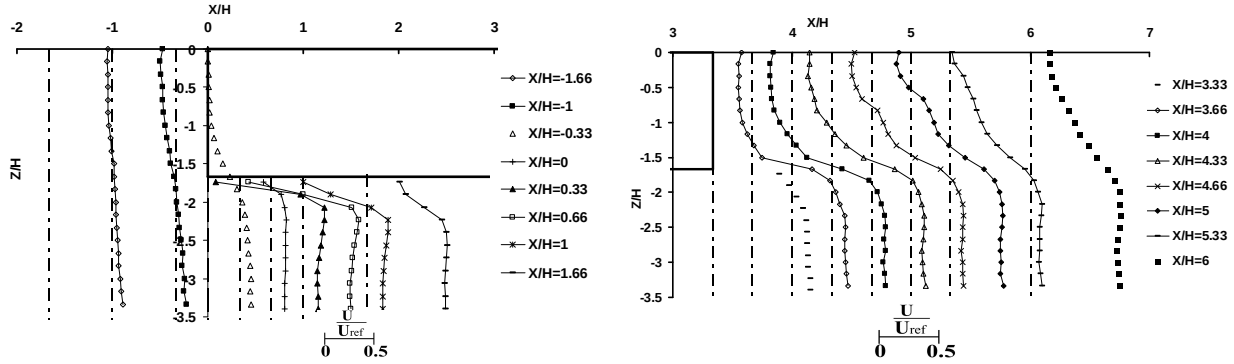

a) X/H<3 b) X/H>3

Fig. 8. Distribution of stream-wise velocity around surface mounted building at a horizontal plane (Y/H=0.5, middle height of the building) for free stream velocity of 10 m/s

Figures 9a and 9b show the turbulence intensity at the horizontal plane of Y/H=0.5. The experimental data shows that the RMS of velocity fluctuation in stream-wise direction increases approaching from the free stream to the building front and side walls. At the back of the building the turbulence intensity has the maximum value at the outer of reverse flow region.

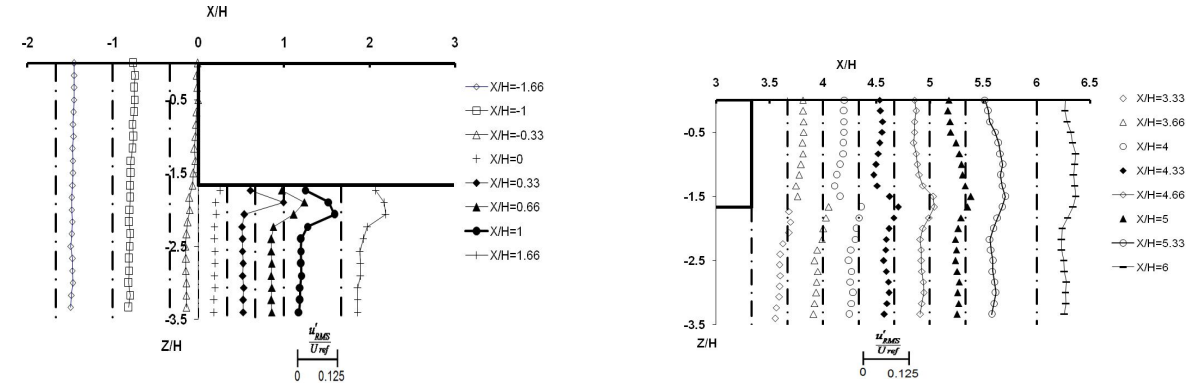

a) X/H<3 b)X/H<3

Fig. 9. Distribution of turbulence intensity around surface mounted building at a horizontal plane (Y/H=0.5, middle height of the building) for free stream velocity of 10 m/s

Figure 10 shows the stream-wise velocity at the symmetry plane for the supported building. Inrush of the flow under the building causes the recirculation zone to totally disappear in front. The stream-wise velocity was decelerated near the building front, which imposes a higher velocity over and under the building. The reattachment length for the recirculation zone on the roof is larger compared with that for the surface mounted building because the stream lines have to turn more sharply on the roof for this case and this enlarges the recirculation zone (X_t/H =1.37). Contrary to the surface mounted case, the velocity gradient is increased, especially on the roof of the supported building.

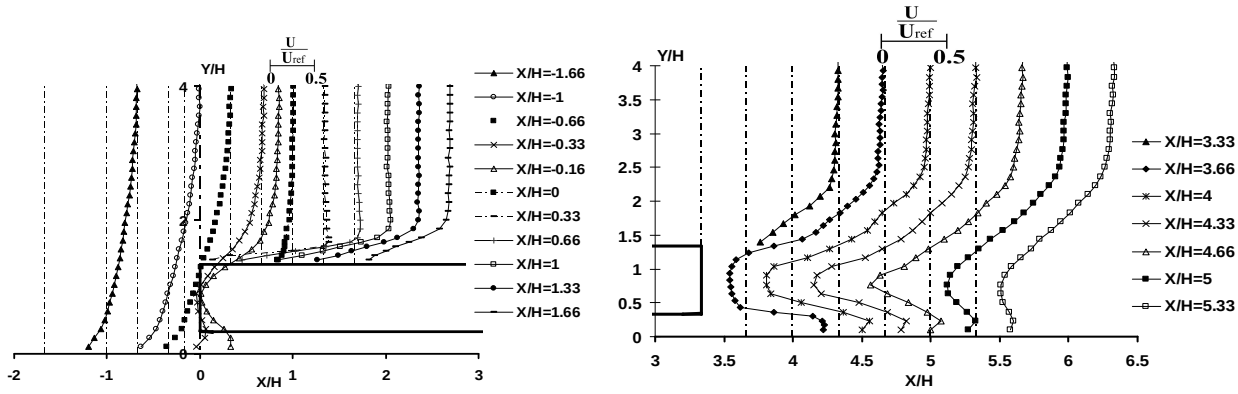

a) X/H<3 b) X/H>3

Fig. 10. Distribution of stream-wise velocity around supported building at the symmetry plane for free stream velocity of 10 m/s

The flow behind the supported case differs considerably compared with that for the surface mounted building. Similar to the pattern observed in front of the building, in all plotting lines a major defect can be seen. Flow under supported case exits with a maximum velocity of nearly 5.2m/s. Also, two counter rotating vortices occur in the recirculation zone at the back of the building and the length of this zone (X_r/H=1.43) is smaller compared with that for the one mounted on the surface. Table 1 compares the sizes of the recirculation zones for surface mounted and supported buildings at the front, top and back of the models. As the height of boundary layer, turbulence intensity and aspect ratio affect the reattachment length and the velocity profiles of both types of the studied building, the earlier experimental data with a different condition could not be used for comparison. However, in the earlier numerical work of the present authors [28] the flow around the same surface mounted building was investigated using large eddy simulation technique. The reattachment lengths at the top and back of the building predicted in the mentioned numerical work are compared with the present experimental data in Table 1, and close agreement is obtained.

Table 1. Reattachment lengths for surface mounted and supported buildings.

Type of building	X_f/H	X_t/H	X_r/H
Surface mounted	1	0.533	2.44
LES model for surface mounted [28]	1.17	0.64	2.43
Supported	0	1.37	1.43

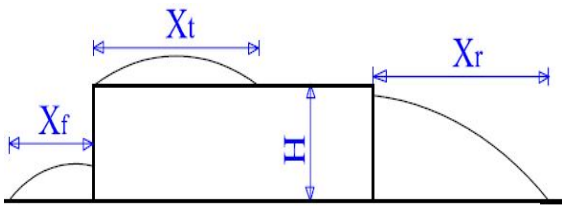

For better comparison of the flow around supported and surface mounted buildings, the stream-wise and fluctuation velocities measured at the middle height of supported building (Y/H=0.833) are shown in Fig. 11. Near the side of supported building, the flow has a higher velocity compared with the free stream velocity which causes a higher gradient in the stream-wise velocity profile and increases the reattachment length compared with that for surface mounted building.

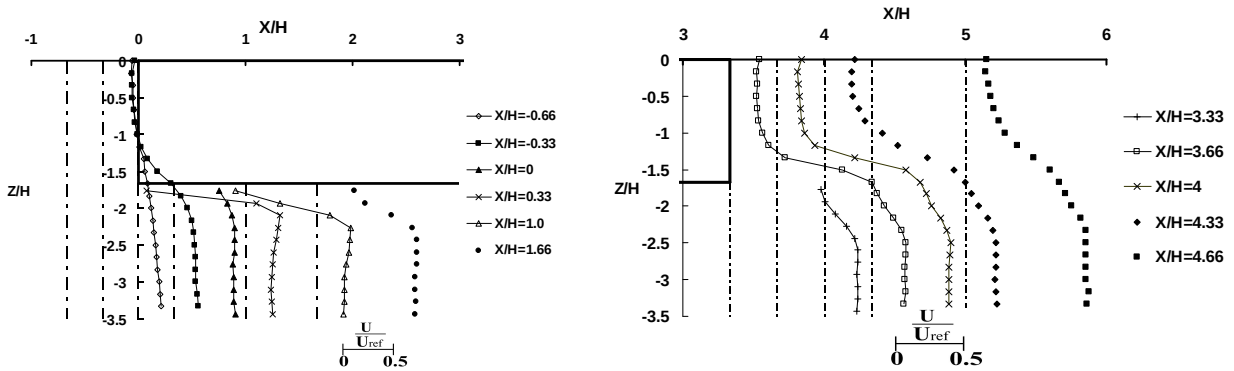

a) X/H<3 b) X/H>3

Fig. 11. Distribution of stream-wise velocity around supported building at a horizontal plane (Y/H=0.833, middle height of the building) for free stream velocity of 10 m/s

The maximum turbulence intensity around the supported building occurs at the locations of maximum velocity gradient (Fig. 12 and Fig. 13). Contrary to the surface mounted building, approaching the building front, turbulence intensity decreases. Although at the back of the supported one the maximum value of turbulence intensity is roughly equal to that for the surface mounted building, but the existence of two relative maximum gradients causes a different trend in the profile of the turbulent intensity.

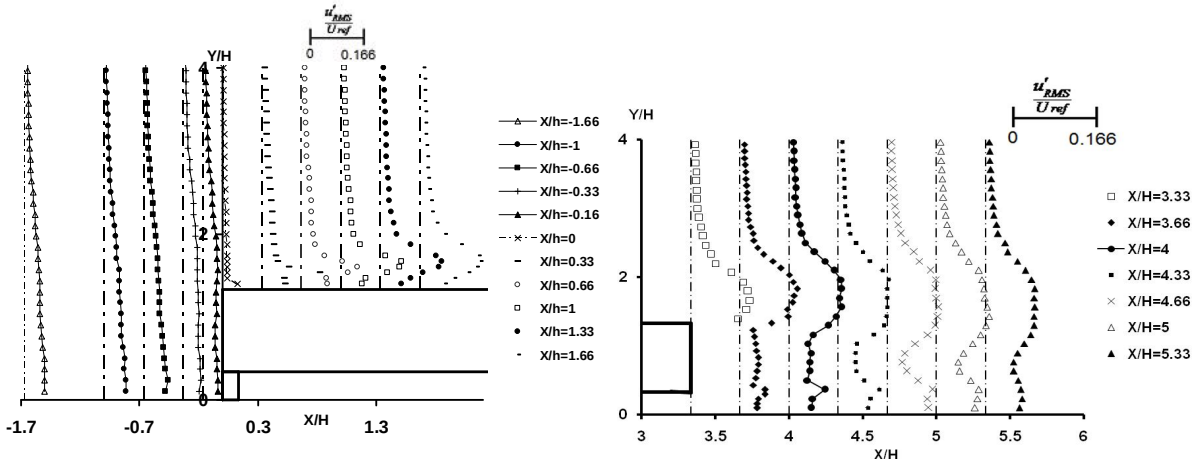

a) X/H<3 b) X/H>3

Fig. 12. Distribution of turbulence intensity around supported building at the symmetry plane for free stream velocity of 10 m/s

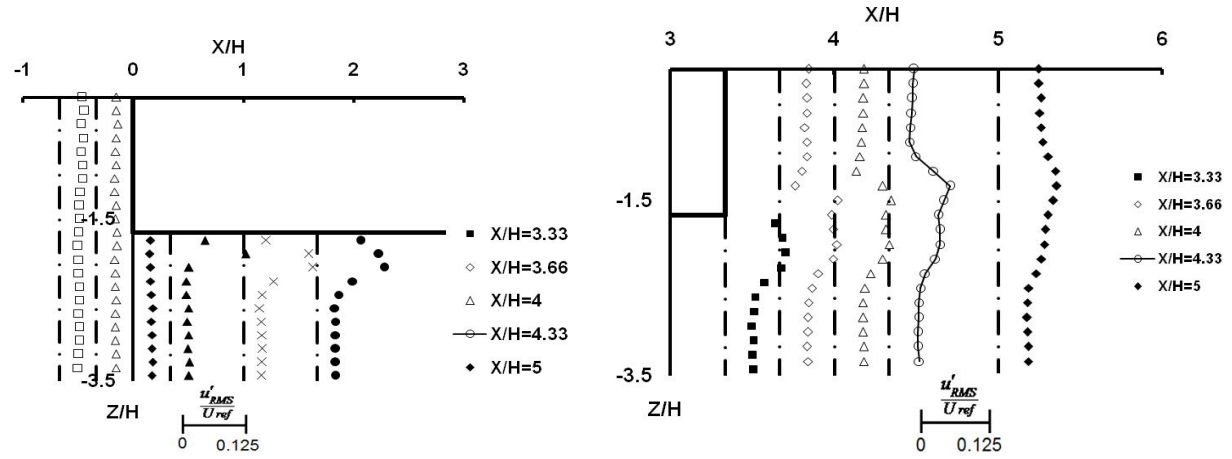

a) X/H<3 b)X/H>3

Fig. 13. Distribution of turbulence intensity around supported building at a horizontal plane (Y/H =0.833, middle height of the building) for free stream velocity of 10 m/s

4. CONCLUSION

The mean and fluctuation stream-wise velocities were measured around two models of supported and surface mounted buildings in the wind tunnel. The following conclusions can be mentioned on the basis of experimental results:

1) Contrary to surface mounted buildings, no recirculation zone was observed in front of supported building. But the reattachment length on the roof increases compared with that of surface mounted building. Also, the recirculation zone behind the supported building is smaller and includes two vortices circulating in opposite directions.
2) The experimental data depict that in the upstream, supported building imposes higher turbulence intensity but at the downstream, the trend is reversed and the flow around surface mounted building has higher turbulence intensity.

NOMENCLATURE

d	cylinder diameter
F	non-dimensional frequency
f	vortex frequency
H	height of building
Re	Reynolds number
U	mean velocity component in the x direction
u'_{RMS}	root mean square of velocity fluctuation in the x direction
U_{ref}	reference value of velocity
X_f, X_t , X_r	reattachment length at the front , top and behind of the building
X, Y, Z	directions of Cartesian coordinate system
y	position in Y direction

Greek Symbols

ν	kinematic viscosity
δ	height of boundary layer

REFERENCES

1. Chand, I., Bhargavain, P. & Krishaki, L.V. (1998). Effect of balconies on ventilation inducing aeromotive force on low-rise buildings. *J. Build Environ.*, Vol. 33, pp. 385-396.
2. Ginger, J. D. & Holmes, J. D. (2003). Effect of building length on wind loads on low-rise buildings with a steep roof pitch. *J. Wind Eng. Ind. Aerodyn.*, Vol. 91, pp. 1377–1400.
3. Castro, I. P. & Robins, A. G. (1977). The flow around a surface-mounted cube in uniform and turbulent streams. *J. Fluid Mech.*, Vol. 79, pp. 307-335.
4. Zhang, A. & Ming, G. (2008). Wind tunnel tests and numerical simulations of wind pressures on buildings in staggered arrangement, *J. Wind Eng Ind Aerodyn*., Vol. 96, pp. 2067–2079.
5. Li, Q. S., Fu, J. Y., Xiao, Y. Q., Li, Z. N., Ni, Z. H., Xie, Z. N. & Gu , M. (2006). Wind tunnel and full-scale study of wind effects on China's tallest building. *J. Eng. Struct*., Vol. 28, pp. 1745–1758.
6. Reynolds, R.T. & Castro, I. P. (2008). Measurements in an urban-type boundary layer. *J. Exp Fluids*., Vol. 45, pp. 141–156.
7. Faghih, A. K. & Bahadori, M. N. (2009). Experimental investigation of air flow over domed roofs. *Iranian Journal of Science & Technology, Transaction B: Engineering*, Vol. 33, No. B3, pp. 207–216.
8. Meroney, R. N., Leitl, B. M., Rafailidis, S. & Schatzmann, M. (1999). Wind-tunnel and numerical modeling of flow and dispersion about several building shapes. *J. Wind Eng Ind Aerodyn.*, Vol. 81, pp. 333-345.
9. Tominaga, Y., Mochida, A., Murakami, S. & Sawaki, S. (2008). Comparison of various revised k–e models and LES applied to flow around a high-rise building model with 1:1:2 shape placed within the surface boundary layer. *J. Wind Eng Ind Aerodyn*. Vol. 96, pp. 389–411.
10. Townsend, A. A. (1956). *The structure of turbulent shear flow.* Cambridge Univ press, p. 315.
11. Golden, J. (1961). Scale model techniques. M. S. Thesis, College of Engr. New York University.
12. Smith, E. G. (1951). The feasibility of using models for predetermining natural ventilation. *Res. Rep. Tex. Eng. Exp. Stn.*, Vol. 26.
13. Snyder, W. H. (1972). Similarity criteria for the application of fluid models to the study of air pollution meteorology. *J. Boundary Layer Meteorol*., Vol. 3, pp. 113-134.
14. Phillips, J. C., Thomas, N. H., Perkins, R. J. & Miller, P. C. H. (1999). Wind tunnel velocity profiles generated by differentially-spaced flat plates. *J. Wind Eng. Ind. Aerodyn*., Vol. 80, pp. 253-262.
15. Armitt, J. & Counihan, J. (1968). The simulation of the atmospheric boundary layer in a wind tunnel. *J. Atmos. Environ*., Vol. 2, pp. 49-71.
16. Counihan, J. (1969). An improved method of simulating an atmospheric boundary layer in a wind tunnel. *J. Atmos. Environ*., Vol. 3, pp. 197-214.
17. Cook, N. J. (1978). Wind tunnel simulation of the atmospheric boundary layer by roughness, barrier and mixing device methods. *J. Wind Eng. Ind. Aerodyn.*, Vol. 3, pp. 157-176.
18. Meng, T. & Hibi, K. (1998). Turbulent measurements of the flow field around a high-rise building. *J. Wind Engineering and Industrial Aerodynamics J. Wind Eng., Jpn.*, Vol. 76, pp. 55–64 (in Japanese).
19. Yaghoubi, M. & Mahmoodi, S. (2004). Experimental study of turbulent separated and reattached flow over a finite blunt plate. *J. Exp Therm. Fluid Sci*., Vol. 29, pp. 105-112.
20. Tavakol, M. M., Yaghoubi, M. & Masoudi Motlagh, M. (2009). Air flow aerodynamic on a wall mounted hemisphere for various turbulent boundary layers. *J. Exp Therm Fluid Sci*., Vol. 34, pp. 538-553.
21. Dantec dynamics. Probes for hot-wire anemometry**,** www.dantecdynamics.com
22. Roshko, A. (1954). On the development of the turbulent wakes from vortex streets. NACA Report, p. 1191.
23. Ardekani, M. A. (2009). Hot-wire calibration using vortex shedding. *J. Measurement.*, Vol. 42, pp. 722–729.

24. Martinuzzi, R. & Havel, B. (2000). Turbulent flow around two interfering surface-mounted cubic obstacles in tandem arrangement. *J. Fluids Eng*., Vol. 122, No. 24, http://dx.doi.org/10.1115/1.483222 (8 pages).
25. Havel, B., Hangan, H. & Martinuzzi, R. (2001). Buffeting for 2D and 3D sharped-edge bluff bodies. *J. Wind Eng. Ind. Aerodyn.*, Vol. 89, pp. 1369-1381.
26. Durbin, P. A. (1996). On the k–e stagnation point anomaly. *J. Heat Fluid Flow*, Vol. 17, pp. 89–90.
27. Martinuzzi, R. & Tropea, C. (1993). The flow around surface mounted, prismatic obstacles placed in a fully developed channel flow. *J. Fluids Eng.*, Vol. 115, pp. 85–93.
28. Motallebi Hasankola, S. S. & Abouali, O. (2010). Numerical investigation of the flow field around a low rise building using les technique. ASME 2010 3rd Joint US-European Fluids Engineering Summer Meeting, http://dx.doi.org/10.1115/FEDSM-ICNMM2010-30739.